Static Magnetic Order in Metallic $K_{0.49}CoO_2$

J. Sugiyama,[1,*] H. Nozaki,[1] Y. Ikedo,[1] K. Mukai,[1] J. H. Brewer,[2] E. J. Ansaldo,[3] G. D. Morris,[3] D. Andreica,[4,5] A. Amato,[5] T. Fujii,[6] and A. Asamitsu[6]

[1]Toyota Central Research and Development Labs, Inc., Nagakute, Aichi 480-1192, Japan
[2]TRIUMF, CIAR and Department of Physics and Astronomy, University of British Columbia, Vancouver, BC, V6T 1Z1 Canada
[3]TRIUMF, 4004 Wesbrook Mall, Vancouver, BC, V6T 2A3 Canada
[4]Faculty of Physics, Babes-Bolyai University, 3400 Cluj-Napoca, Romania
[5]Laboratory for Muon-Spin Spectroscopy, Paul Scherrer Institut, Villigen PSI, Switzerland
[6]Cryogenic Center, University of Tokyo, 2-11-16 Yayoi, Bunkyo-ku, Tokyo 113-0032, Japan
(Received 27 October 2005; published 27 January 2006)

By means of muon-spin spectroscopy, we have found that $K_{0.49}CoO_2$ crystals undergo successive magnetic transitions from a high-T paramagnetic state to a magnetic ordered state below 60 K and then to a second ordered state below 16 K, even though $K_{0.49}CoO_2$ is metallic at least down to 4 K. An isotropic magnetic behavior and wide internal-field distributions suggest the formation of a commensurate helical spin density wave (SDW) state below 16 K, while a linear SDW state is likely to exist above 16 K. It was also found that $K_{0.49}CoO_2$ exhibits a further transition at 150 K presumably due to a change in the spin state of the Co ions. Since the T dependence of the internal-field below 60 K was similar to that for $Na_{0.5}CoO_2$, this suggests that magnetic order is more strongly affected by the Co valence than by the interlayer distance or interaction and/or the charge ordering.

DOI: 10.1103/PhysRevLett.96.037206 PACS numbers: 75.30.Fv, 72.15.Jf, 75.30.Kz, 76.75.+i

The Na_xCoO_2 (NCO) system has emerged recently as a new paradigm of low-dimensional, strongly correlated systems because of its direct relevance to several condensed matter topics of great current interest, primarily enhanced thermopowers [1], frustrated magnetic ordering in triangular lattices [2], and unconventional superconductivity [3]; and the possible fundamental interrelationship between those properties, which can be studied as a function of doping as the rich but complex NCO phase diagram, is explored further [4,5]. In particular, magnetic and superconducting order parameters are based on the CoO_2 planes, as for the cuprates, with interlayers playing a crucial role for the doping and couplings. In the NCO case mobility and inhomogeneity of the Na^+ ions may lead to extra difficulties in the interpretation of experimental results on magnetic ordering, especially in the metallic region for $x \geq 0.7$. In addition, and in contrast to the cuprates, the spin-charge dynamics of the Co ions in the plane play a major role which needs to be understood better, by further studies.

Since NCO is a member of the family A_xCoO_2 ($A =$ Li, Na, K, Rb, and Cs), and other members also display interesting and complex magnetic orderings depending on the average Co valence of the CoO_2 planes (V_{Co}), we have initiated its systematic study with positive muon-spin rotation and relaxation (μ^+SR) spectroscopy. Results for $A =$ Li and $x = 1$ were reported recently [6], and in this Letter we wish to report the appearance of successive ordering transitions to quasistatic (i.e., static at least for muon's life time, 2.2 μs) bulk magnetic states in $K_{0.49}CoO_2$, and in contrast lack of magnetic order above 5 K for $Rb_{0.3}CoO_2$. Both $K_{0.49}CoO_2$ and $Rb_{0.3}CoO_2$ crystals exhibit metallic conductivity down to 4 K with nearly T independent susceptibility (χ), while the $\chi(T)$ curve of the two crystals showed a small increase below ~20 K for reasons unknown [7]. It is thus believed that both compounds are Pauli paramagnets down to 4 K.

For the cobaltites with $V_{Co} \leq 3.4$, we have previously proposed a universal dome-shaped magnetic phase diagram not only for NCO but also for more complex layered cobaltites [2,4]. Very recently, the dome shape was reconfirmed by the μ^+SR experiments on $Na_{0.85}CoO_2$ and $NaCoO_2$ [8,9], although T_N for $Na_{0.85}CoO_2$ seems to be a little higher than that predicted by a smooth dome function, perhaps due to structural changes over a narrow range of x for NCO. This leads to the question of what are the common intrinsic features for all layered cobalt oxides in the V_{Co} range above 3.4. In particular, $V_{Co} \sim 3.5$ is worth investigating, because $Na_{0.5}CoO_2$ was reported to enter into a charge ordered insulating state below 83 K and/or 53 K, by χ and resistivity (ρ) measurements [5]. Also, μ^+SR on $Na_{0.5}CoO_2$ showed the appearance of quasistatic magnetic order below 83 K, for which several spin-precession signals were detected [8]. The origin of magnetism was naturally explained using the concept of charge ordering in the CoO_2 plane.

High quality single-crystal platelets of $K_{0.49}CoO_2$ were grown at the University of Tokyo by a flux technique using reagent grade K_2CO_3 and Co_3O_4 powders as starting materials. A mixture of KCl, K_2CO_3, and B_2O_3 was used as the flux. The typical dimension of the obtained $K_{0.49}CoO_2$ platelets was $\sim 3 \times 3 \times 0.05$ mm^3. The composition of the platelets was determined by an induction coupled plasm analysis. The preparation and characterization of these crystals were reported in greater detail elsewhere [7]. In order to stop muons in the sample and to increase the signal

 © 2006 The American Physical Society

intensity, ~30 platelets were stacked in a muon-veto sample holder. The μ^+SR experiments were performed on the surface muon beam line of **M20** at TRIUMF and π**M3** (GPS) at PSI. The direction of the spin of the muons relative to the plane of the crystals was set by the spin rotator—Wien filters in the beam lines. The experimental setup and procedures are described elsewhere [10].

Figure 1 shows zero-field (ZF-)μ^+SR time spectra at 1.7 K for single-crystal platelets of $K_{0.49}CoO_2$. The top spectrum was obtained with the initial μ^+ spin direction $\mathbf{S}_\mu(0)$ parallel to the a axis and the bottom one with $\mathbf{S}_\mu(0)$ parallel to c. A clear oscillation due to quasistatic internal fields $\boldsymbol{H}_{\rm int}$ is observed in both cases, indicating an isotropic magnetic structure in $K_{0.49}CoO_2$. This behavior is very different from the large magnetic anisotropy observed in the other layered cobaltites, such as $Na_{0.9}CoO_2$, $[Ca_2CoO_3]_{0.62}[CoO_2]$, and $[Ca_2Co_{4/3}Cu_{2/3}O_4]_{0.62}[CoO_2]$ [2,11]. The signal is fitted best by three exponentially relaxed cosine oscillations with the same initial phase, which describe three different muon sites in a commensurate $\boldsymbol{H}_{\rm int}$ distribution.

Figure 2 shows the change in the Fourier transform of the ZF-μ^+SR time spectrum as a function of T. At the lowest T measured, the spectrum consists of three main peaks at around 0.8, 1.1, and 1.5 MHz with additional small peaks, although to the eye the spectrum seems to be a main broad peak with several minor peaks, which is due to a wide distribution of $\boldsymbol{H}_{\rm int}$ in $K_{0.49}CoO_2$. This reflects the appearance of a commensurate spin density wave (C-SDW) order, as predicted by the calculation using a Mott-Hubbard model, discussed later.

As T increases from 1.63 K, the peak at 0.8 MHz shifts towards a lower frequency, and then seems to disappear at ~20 K, while the other two peaks (at 1.1 and 1.5 MHz) are roughly T independent. The spectrum drastically changes its shape at 20 K with further increasing T. That is, the fast-Fourier-transform (FFT) spectrum consists of two sharp peaks above 20 K, showing that the field distribution above 20 K is narrower than below 20 K. In other words, this indicates a change in the magnetic structure probably due to a transition around 20 K. The frequencies of both peaks decrease with further increasing T up to ~60 K.

Figures 3(a) and 3(b) show the T dependence of the muon precession frequencies ($\nu_{\mu,i} = \omega_{\mu,i}/2\pi$) and χ for the single-crystal platelets of $K_{0.49}CoO_2$. According to the T dependence of the FFT, as T increases from 1.63 K, $\nu_{\mu,2}$ is roughly T independent, while $\nu_{\mu,1}$ and $\nu_{\mu,3}$ decrease monotonically with increasing T up to ~16 K. Then, the lowest $\nu_{\mu,3}$ disappears, while $\nu_{\mu,1}$ and $\nu_{\mu,2}$ suddenly decreases by about 0.3 MHz. With further increase of T, the two frequencies decrease monotonically with increasing slope ($d\nu_\mu/dT$) and disappear at ~55 K. This behavior is quite consistent with the $\chi(T)$ curve, which exhibits a small peak at 55 K and a rapid increase below 20 K. Also, the $\chi(T)$ curve measured in zero-field-cooling (ZFC) mode starts to deviate from that in field-cooling (FC) mode below 20 K. We therefore conclude that $K_{0.49}CoO_2$ undergoes a transition from a paramagnetic to a magnetically ordered state at $T_{C,1} = 55$ K and then to the other ordered state at $T_{C,2} \sim 16$ K.

Although neutron diffraction experiments are the most powerful technique to determine the magnetic structures of the two phases, the current μ^+SR results provide primary information on them. First, there are no indications of charge ordering in the $\rho(T)$ and $\chi(T)$ curve for $K_{0.49}CoO_2$, in contrast to both $Na_{0.5}CoO_2$ and $K_{0.5}CoO_2$ [12]. This suggests that the commensurate, three-sublattice, 120° twisted SDW state is most unlikely to exist

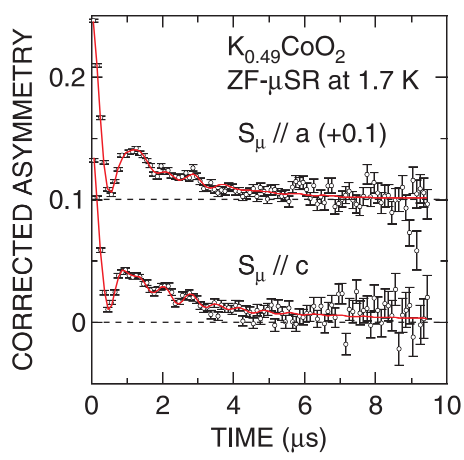

FIG. 1 (color online). ZF-μ^+SR time spectra of single-crystal platelets of $K_{0.49}CoO_2$ at 1.7 K. The configurations of the sample and the initial muon-spin direction $\mathbf{S}_\mu(0)$ are (top) $\mathbf{S}_\mu(0) \parallel \mathbf{a}$ and (bottom) $\mathbf{S}_\mu(0) \parallel \mathbf{c}$. The top spectrum is offset by 0.1 for clarity of the display.

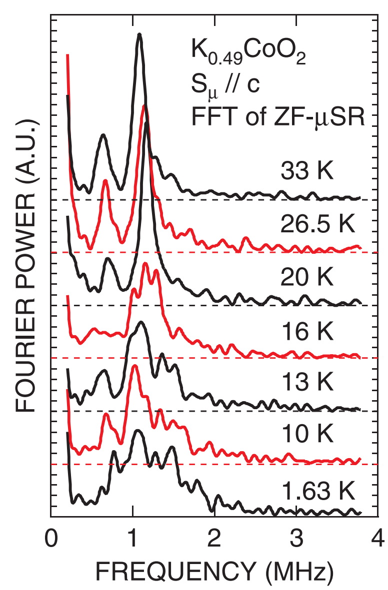

FIG. 2 (color online). Temperature dependence of the Fourier transform of the ZF-μ^+SR time spectrum for $K_{0.49}CoO_2$. Here, the ZF-μ^+SR spectrum was obtained using $\mathbf{S}_\mu(0) \parallel \mathbf{c}$ configuration.

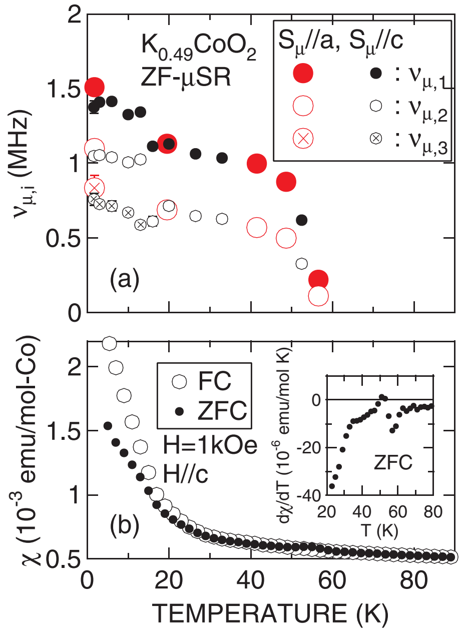

FIG. 3 (color online). Temperature dependence of (a) muon precession frequency $\nu_{\mu,i}$ and (b) dc susceptibility χ for $K_{0.49}CoO_2$. The data of $\nu_{\mu,i}$ were obtained by fitting the ZF spectrum with three exponentially relaxed cosine oscillation signals with the same initial phase. Large circles represent the data obtained with $\mathbf{S}_\mu(0) \parallel \mathbf{a}$ configuration at TRIUMF, and the small circles with $\mathbf{S}_\mu(0) \parallel \mathbf{c}$ configuration at PSI. Both measurements were carried out using different batches of crystals. χ was measured in both zero-field-cooling *ZFC* and field-cooling *FC* mode with $H = 1$ kOe. The inset of (b) shows the T dependence of the slope of χ ($d\chi/dT$) measured in *ZFC*.

in $K_{0.49}CoO_2$, because the 120° antiferromagnetic (AF) domain structure, which is the ground state for the classical AF triangular lattice, naturally induces an insulating state. Second, the isotropic behavior observed by the ZF-μ^+SR measurements clearly precludes in this case the possibility of the A-type AF—i.e., ferromagnetic (FM) order in the CoO_2 plane but AF between the adjacent two CoO_2 planes, which was proposed for $Na_{0.82}CoO_2$ [13].

In order to explain magnetism on the two-dimensional triangular lattice, the Hubbard model within a mean field approximation has been applied using the Hamiltonian $\mathcal{H}$ given by [14,15]

$$\mathcal{H} = -t\sum_{\langle ij\rangle\sigma} c_{i\sigma}^{\dagger} c_{j\sigma} + U\sum_{i} n_{i\uparrow}n_{i\downarrow}, \qquad (1)$$

where $c_{i\sigma}^{\dagger}(c_{j\sigma})$ creates (destroys) an electron with spin σ on site i, $n_{i\sigma} = c_{i\sigma}^{\dagger}c_{i\sigma}$ is the number operator, t is the nearest-neighbor hopping amplitude, and U is the Hubbard on-site repulsion. The electron filling n is defined as $n = (1/2N)\sum_i^N n_i$, where N is the total number of sites.

Since decrease in the K content (x) produces holes in K_xCoO_2, $x = 0.49$ corresponds to $n = 0.255$, if we ignore oxygen deficiency in the sample. As n decreases from 0.5, the calculations predict that the linear (L) SDW phase transforms into the helical (H) SDW phase at around $n = 0.4$ for $4.4 \leq U/t \leq 4.8$. For the LSDW phase, a zigzag FM chain is formed and neighboring FM chains align antiferromagnetically (see Fig. 4) [16], while Co spins form a helical structure in the plane for the HSDW phase.

In the LSDW state, as seen in Fig. 4, two possible muon sites, one just above/below the corner of the triangular lattice and the other at the center of the triangular lattice, originate the two different ν_μs, corresponding to the two sharp peaks in the FFT above 20 K. In the HSDW state, however, the helical spin structure produces a wide field distribution at the muon sites. In other words, the LSDW state is most likely to appear below 55 K, and then the HSDW state below ~16 K.

In order to elucidate the magnetic behavior above 55 K, we performed weak-transverse-field (wTF-) μ^+SR measurements up to 300 K, with the results shown in Fig. 5 together with χ^{-1} and ρ. Besides the two transitions at 55 K and 20 K, both the slope of the wTF-relaxation rate (λ_{TF}) and the normalized wTF-oscillation frequency ($\Delta\omega_\mu$) show an anomaly at ~150 K, where the $\chi^{-1}(T)$ curve exhibits a broad maximum. Above 60 K, the wTF asymmetry (A_{TF}) levels off to its maximum value (~0.2)—i.e., the sample volume is almost 100% paramagnetic. This therefore suggests that the changes in λ_{TF} and $\Delta\omega_\mu$ are due to a spin state transition. The other possibility, a charge ordering of Co^{3+} and Co^{4+}, is most unlikely to occur, because the $\rho(T)$ curve shows no anomalies around 150 K. A spin state transition was also proposed for $PrCoO_3$ [17], for which the $\chi^{-1}(T)$ curve exhibits a broad maximum around 200 K.

The wTF-μ^+SR results also provide an insight for the ordered state. The monotonic decrease in the A_{TF} below 55 K (and the accompanying increase in A_{fast}) indicates that the magnetic order develops gradually with decreasing T due to geometrical frustration of the triangular lattice. Actually, the $A_{TF}(T)$ curve does not level off at the lowest T measured. The volume fraction of the magnetic phase extrapolated to 0 K is estimated as ~80%.

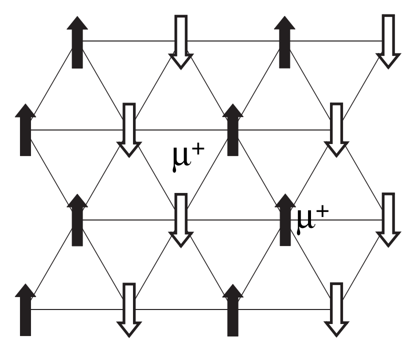

FIG. 4. Spin structure of a linear spin density wave (LSDW) state on the two-dimensional triangular lattice. Two possible muon sites (μ^+), which locate not in the Co plane but in the oxygen plane and are surrounded by three O^{2-} ions, are shown. These two sites are more preferable than the sites between the edge of the triangle, which are surrounded by two O^{2-} ions.

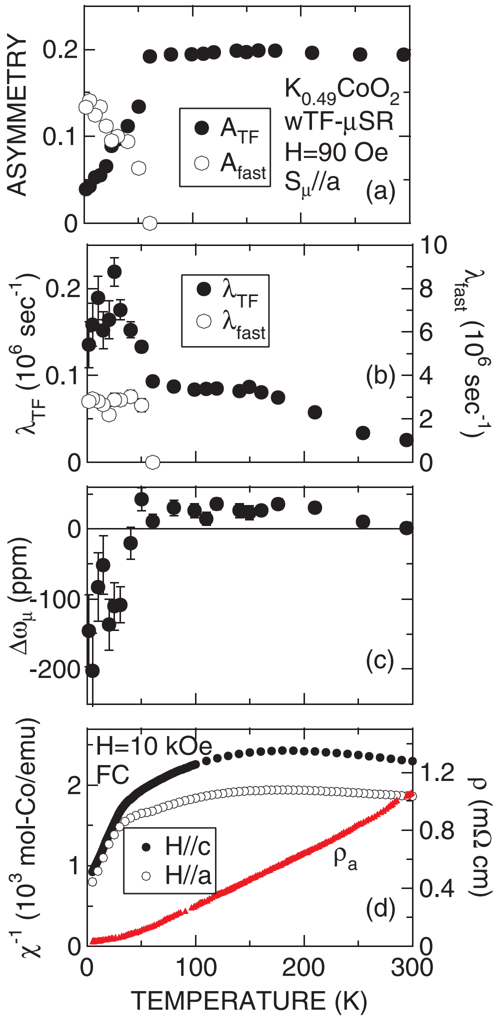

FIG. 5 (color online). Temperature dependences of (a) A_{TF} and A_{fast}, (b) λ_{TF} and λ_{fast} and (c) the shift of the muon precession frequency, $\Delta\omega_\mu$, and (d) the inverse susceptibility, χ^{-1} and resistivity, ρ [7] in $K_{0.49}CoO_2$ crystals. The data were obtained by fitting the wTF-μ^+SR spectra with a combination of a slowly relaxing precessing signal due to the external field and a fast nonoscillatory signal caused by the internal fields; $A_{TF}\exp(-\lambda_{TF}t)\cos(\omega_\mu t + \phi) + A_{fast}\exp(-\lambda_{fast}t)$.

It should be noted that the overall T dependence of $\nu_{\mu,i}$ for $K_{0.49}CoO_2$ is very similar to that for the $Na_{0.5}CoO_2$ sample [8]. Since in that experiment the sample was polycrystalline and the data reported only below 90 K, there was no information on possible magnetic anisotropy or a spin state transition. This therefore raises the question concerning the origin of the magnetic order in $Na_{0.5}CoO_2$. Although alkali ions become more ionic with increasing atomic number, there are almost no contributions to the shape of the electronic structure, but just producing holes, even for NCO [18]. The main difference between NCO and $K_{0.49}CoO_2$ is hence the change in the interlayer distance of the two adjacent CoO_2 planes and as a result the decrease in the interlayer interaction.

The present results indicate that magnetism in the layered cobaltites with $V_{Co} \sim 3.5$ is not strongly affected by interlayer distance or interaction and the charge ordering but by V_{Co}. In other words, the phase diagram proposed for NCO [5] is likely to be applicable to the other A_xCoO_2, if the x region of the magnetic order is extended. Additionally, we have performed μ^+SR measurements on $Rb_{0.3}CoO_2$, which showed the absence of magnetism down to 5 K. The ZF-μ^+SR spectra in that case are well described by a dominant static Kubo-Toyabe function with the field distribution $\Delta \sim 0.2 \times 10^6$ s^{-1} at 5 K, implying that the muons experience interactions only with the spins of Co and Rb nuclei in a paramagnetic state, similar to $Na_{0.35}CoO_2$ [19]. This further supports the similarity among the A_xCoO_2 family. We wish finally to mention that, if the K/A content is controlled precisely, better thermoelectrics and even new superconductors are also likely to be found in A_xCoO_2.

This work was performed at both TRIUMF and PSI. We thank S. R. Kreitzman, B. Hitti, D. J. Arseneau of TRIUMF, P. Russo of Columbia University and the LMU staff of PSI for help with the μ^+SR experiments, and Y. Kawai of Toyota CRDL for the ICP analysis. This work was partially (J. H. B.) supported at UBC by CIAR, NSERC of Canada, and at TRIUMF by NRC of Canada.

*Electronic address: e0589@mosk.tytlabs.co.jp

[1] I. Terasaki, Y. Sasago, and K. Uchinokura, Phys. Rev. B **56**, R12685 (1997).
[2] J. Sugiyama *et al.*, Phys. Rev. B **67**, 214420 (2003); **69**, 214423 (2004).
[3] K. Takada *et al.*, Nature (London) **422**, 53 (2003).
[4] J. Sugiyama *et al.*, Phys. Rev. Lett. **92**, 017602 (2004).
[5] M. L. Foo *et al.*, Phys. Rev. Lett. **92**, 247001 (2004).
[6] J. Sugiyama *et al.*, Phys. Rev. B **72**, 144424 (2005).
[7] T. Fujii *et al.*, in The Meeting Abstracts of Physical Society of Japan **60**, No. 2, 561 (2005) (in Japanese).
[8] P. Mendels *et al.*, Phys. Rev. Lett. **94**, 136403 (2005).
[9] G. Lang *et al.*, Phys. Rev. B **72**, 094404 (2005).
[10] G. M. Kalvius, D. R. Noakes, and O. Hartmann, *Handbook on the Physics and Chemistry of Rare Earths*, edited by K. A. Gschneidner, Jr., L. Eyring, and G. H. Lander (North-Holland, Amsterdam, 2001), Vol. 32, Chap. 206.
[11] J. Sugiyama *et al.*, Phys. Rev. B **68**, 134423 (2003); J. Phys. Condens. Matter **15**, 8619 (2003).
[12] N. Mori *et al.*, in The Meeting Abstracts of Physical Society of Japan **60**, No. 1, 485 (2005) (in Japanese).
[13] S. P. Bayrakci *et al.*, Phys. Rev. Lett. **94**, 157205 (2005).
[14] H. R. Krishnamurthy *et al.*, Phys. Rev. Lett. **64**, 950 (1990).
[15] M. Fujita, M. Ichimura, and K. Nakao, J. Phys. Soc. Jpn. **60**, 2831 (1991); M. Fujita, T. Nakanishi, and K. Machida, Phys. Rev. B **45**, 2190 (1992).
[16] C. Jayaprakash *et al.*, Europhys. Lett. **15**, 625 (1991).
[17] J.-Q. Yan *et al.*, Phys. Rev. B **69**, 134409 (2004).
[18] D. J. Singh, Phys. Rev. B **61**, 13 397 (2000).
[19] I. R. Mukhamedshin *et al.*, Phys. Rev. Lett. **94**, 247602 (2005).